[PROC. OF JSCE No. 387/II-8 (Hydraulic and Sanitary Eng.) November 1987]

ADAPTIVE FINITE ELEMENT METHOD FOR LINEAR WATER WAVE PROBLEMS

By Kazuo KASHIYAMA and Mutsuto KAWAHARA***

This paper presents a finite element method for the analysis of linear water wave problems using the mesh optimization technique. The numerical model is based on the mild-slope equation. The hybrid element method is employed for the numerical treatment of the open boundary. The key feature of this method is that the approximation error based on the finite element discretization is estimated and the finite element mesh is redivided to minimize the total amount of the error. This follows that the accuracy of the numerical solutions is improved automatically. The numerical solutions obtained are compared with analytical solutions. The present method is shown to be an useful and effective method for the analysis of linear water wave problems.
Keywords : *adaptive mesh refinement, hybrid element method, interpolation error, mild slope equation*

1. INTRODUCTION

The numerical analysis of water surface wave problems becomes more important, since the demands of the planning and construction of various offshore and coastal structures increase in recent years. Various numerical methods have been presented by numerous investigators over the years[1)~7)]. The principal object of all of the conventional numerical studies were how to get solutions for the given boundary value problems. As the geometrical shape and boundary conditions become more complicated, a new problem comes into question. That is, it is difficult to measure the accuracy of the numerical solutions since exact solutions cannot be obtained in most cases. In case that there are experimental or observed data, it is possible to compare the numerical solution with the resulted data. However, the fact that numerical solutions agree with exact solutions and the fact that those agree with experimental or observed data are entirely different in the engineering sense. Numerical solutions must well approximate exact solutions strictly. Therefore, it is wholly demanded to establish the method to measure the accuracy of the numerical solutions.

The adaptive finite element method is presented in recent years[8),12)~18)]. This method estimates the approximation error based on the finite element discretization in each element, and redivides the finite element mesh to minimize the total amount of the error. It follows that the accuracy of numerical solutions is improved automatically. Consequently, the adaptive finite element method can overcome the problem how to measure the accuracy of the numerical solutions. Adaptive finite element methods are roughly

* Member of JSCE, Dr. Eng., Research Associate, Department of Civil Engineering, Hiroshima Institute of Technology (Miyake 725, Itsukaichi, Saeki-ku, Hiroshima 731-51)
** Member of JSCE, Dr. Eng., Professor, Department of Civil Engineering, Chuo University (Kasuga 1 chome, Bunkyo-ku, Tokyo 112)

classified into three methods, namely, r-[12)~15)], h-[16),17)], and p-method[15),18)]. The features of each method are as follows. The r-method relocates the nodal points according to the distribution of the estimated approximation error. As a result nodal points gather around the element where approximation error is large. The total number of finite elements and nodal points are unchanged in the r-method. The h-method refines the finite element mesh in which approximation error is large. The total number of finite elements and nodal points increase in the h-method. In the p-methed, higher order finite element approximation is applied to the element in which approximation error is large.

This paper presents an adaptive finite element method based on the r-method for the analysis of linear water wave problems. The mild-slope equation is used for basic equation. The finite element method based on linear triangular element is used for the discretization. For the numerical treatment of infinite boundary, the hybrid element method is employed. Several numerical tests have been performed to show the validity of the present method. The computed results are compared with the analytical solutions. It has been clearly shown that the present method is efficient for the analysis of linear water wave problems.

2. BASIC EQUATION

Assuming the steady state surface waves with infinitesimal amplitude on slowly varying water depth, the surface displacement η may be described by the mild-slope equation[1),9)~11)].

$$(CC_g\eta_{,i})_{,i}+\omega^2(C_g/C)\eta=0 \quad \text{in} \quad \Omega \qquad (1)$$

where Ω denotes wave field, C is phase velocity, C_g is group velocity, and ω is angular frequency. These values are determined by the dispersion relation.

$$\omega^2=gk\tanh kh \qquad (2)$$

where g is gravity acceleration, k is wavenumber and h is water depth.

The surface displacement η is assumed to be the sum of the incident wave η_{in} and scattered wave η_{sc} as :

$$\eta=\eta_{in}+\eta_{sc} \qquad (3)$$

where η_{in} is given as follows :

$$\eta_{in}=A\sum_{n=0}^{\infty}\varepsilon_n\hat{i}^nJ_n(kr)\cos n(\theta-\theta_{in}) \qquad (4)$$

in which A denotes incident wave amplitude, ε_n is Neuman number, $\hat{i}$ is the imaginary unit, J_n is the Bessel function of order n and θ_{in} is incident wave angle, respectively.

As the boundary conditions, the following conditions are introduced on the boundary (see Figure 1) :

$$\eta_{,n}=\partial\eta/\partial n=\gamma\eta \quad \text{on} \quad \Gamma_s \qquad (5)$$

$$\lim_{\gamma\to\infty} r^{\frac{1}{2}}(\eta_{sc,r}-\hat{i}k\eta_{sc})=0 \quad \text{on} \quad \Gamma_\infty \qquad (6)$$

where n means the normals to the boundary, r is the distance from structures, Γ_s is the boundary of structures and Γ_∞ is the artificial infinite boundary. And γ can be expressed in terms of the reflection coefficient as[7)] :

$$\gamma=-\hat{i}k(1-K_r)/(1+K_r) \qquad (7)$$

where K_r denotes the reflection coefficient. The fully reflection condition ($K_r=1.0$) was used for all computations in this paper.

The wave field Ω is divided into two domains, one of which is the inner domain Ω_i with arbitrary geometry and variable water depth, and other is the outer domain Ω_0 with constant water depth. On the boundary of Γ_c, the following continuity conditions should be satisfied as :

$$\eta=\bar{\eta}, \quad CC_g\eta_{,n}=CC_g\bar{\eta}_{,n} \quad \text{on} \quad \Gamma_c \qquad (8)$$

where $\bar{\eta}$ denotes the surface displacement in the outer domain.

3. HIBRID ELEMENT METHOD

For the efficient numerical computation, the finite element method is employed in the inner domain Ω_i

and the boundary solutions is introduced in the outer domain Ω_0 to deal with the radiation condition. This method is called as the hybrid element method, which is firstly presented by Chen and Mei[2].

The scattered wave within outer domain $\overline{\eta}_{sc}$ must satisfy the Helmholtz equation and radiation condition. In this case as shown in **Fig. 1**, the scattered wave can be represented by the Fourier-Bessel expansion as :

$$\overline{\eta}_{sc}=\alpha_0 H_0(kr)+\sum_{n=1}^{\infty} H_n(kr)(\alpha_n \cos n\theta+\beta_n \sin n\theta) \quad \cdots\cdots (9)$$

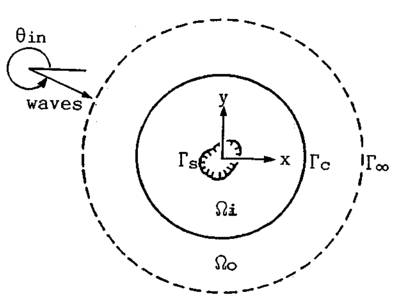

Fig. 1 Definition sketch.

where α_n and β_n denote the unknown constants and H_n is the Hankel function of the first kind of order n.

For the discretization of the spatial variable η, the variational principle can be introduced in the formulation. The variational functional to be minimized for the given boundary value problem is expressed as follows :

$$\Pi=\Pi_i+\Pi_0 \quad \cdots\cdots (10)$$

where

$$\Pi_i=\frac{1}{2}\int_{\Omega_i}[CC_g(\eta_{,i})^2-\omega^2(C_g/C)\eta^2]d\Omega-\int_{\Gamma_S} CC_g\eta\eta_{,n}d\Gamma$$

$$\Pi_0=\int_{\Gamma_C} CC_g\left[\left(\frac{1}{2}\overline{\eta}_{sc}-\eta_{sc}\right)\overline{\eta}_{,n}-\frac{1}{2}\overline{\eta}_{sc}\eta_{in,n}\right]d\Gamma$$

in which Π_i and Π_0 are the variational functional of inner and outer domains respectively.

The linear triangular element is employed for the discretization in inner domain. Minimizing the functional (10), a set of linear complex algebraic equation for surface displacement $\{\eta\}$ can be derived in the following form :

$$[K]\{\eta\}=\{F\} \quad \cdots\cdots (11)$$

where $[K]$ is the stiffness matrix which is to be symmetric and $\{F\}$ is the external source vector involving the incident wave term. Hence, the matrix $[K]$ is stored in a packed form of semi-bandwidth and the band matrix method is employed to solve the equation (11).

4. ADAPTIVE MESH REFINEMENT TECHNIQUE

(1) Optimal Condition of Mesh Optimization Problem[12)~15)]

Denoting the total amount of error TE, an optimization problem can be defined by the following form :

$$\mathrm{Min}_{\mathrm{design}}\, TE \quad \cdots\cdots (12)$$

This equation means that the total amount of error must be minimized in the whole domain. However, it is difficult to estimate the total amount of error TE directly, because the total amount of error can be estimated using the approximation error based on the finite element discretization which is defined in each finite element. Therefore, in order to relate the total amount of error TE to the error of each finite element E_e, the ∞-norm is introduced as follows :

$$TE=\mathrm{Max}_{e=1,\cdots,N_e} E_e \quad \cdots\cdots (13)$$

where e denotes the e-th finite element and N_e is the total number of finite elements.

Introducing equation (13) into (12), the optimal grid design problem should be defined by the min-max concept as :

$$\mathrm{Min}_{\mathrm{design}}\mathrm{Max}_{e=1,\cdots,N_e} E_e \quad \cdots\cdots (14)$$

The necessary condition of equation (14) is easily given as follows :

$$E_e=\mathrm{constant}\,;\ e=1,\cdots,N_e \quad \cdots\cdots (15)$$

Consequently, if the approximation error based on the finite element discretization which is defined in each finite element should be constant in the whole domain, the optimal grid design problem can be accomplished.

(2) The Error Measure in Linear Water Wave Analysis

It is well known that there are two measures of the approximation error based on the finite element discretization, namely, residual[16)~18)] and interpolation error[12)~15)]. In this paper, the interpolation error is used for the error measure.

The wave field in the finite element region is divided into a finite number of elements, and the weak form of finite element equation in each element can be written as follows:

$$a(\eta, \delta\eta)=f(\delta\eta) \quad \cdots\cdots (16)$$

where

$$a(\eta, \delta\eta)=\int_{\Omega_{ie}}[CC_g\eta_{,i}\delta\eta_{,i}-\omega^2(C_g/C)\eta\delta\eta]d\Omega$$

$$f(\delta\eta)=\int_{\Gamma_{se}}CC_g\delta\eta\eta_{,n}d\Gamma$$

in which $\delta\eta$ denotes the variation of η.

The finite element solution is given to satisfy the following equation:

$$a(\eta_h, \delta\eta_h)=f(\delta\eta_h) \quad \cdots\cdots (17)$$

where η_h is the finite element solution.

The measure of the finite element approximation error $e=\eta-\eta_h$ can be defined using the energy norm as:

$$\|e\|=\sqrt{a(e, e)} \quad \cdots\cdots (18)$$

However, it is difficult to evaluate the approximation error directly, since the exact solution η cannot be obtained in most cases. In order to evaluate the approximation error, the interpolation error $e_i=\eta-v_h$ is introduced as follows:

$$\|e_i\|=\sqrt{a(e_i, e_i)} \quad \cdots\cdots (19)$$

where v_h is the interpolation of η. The interpolation error can be evaluated in any cases.

Therefore, the interpolation error in energy norm is used for the error measure, i.e.

$$E_e=\|e_i\|_e=\left\{\int_{\Omega_{ie}}[CC_g((\eta-v_h)_{,i})^2]d\Omega\right\}^{\frac{1}{2}} \quad \cdots\cdots (20)$$

In order to evaluate E_e explicitly, three node triangular element is introduced. Denoting the node $x^\alpha=(x_1^\alpha, x_2^\alpha)$, the following equation is defined from the property of the interpolation function v_h.

$$v_h(x^\alpha)=\eta(x^\alpha) \quad \cdots\cdots (21)$$

Applying the Taylor's expansion, the following equation can be derived as:

$$\eta(x^\alpha)=\eta(x)+\sum_{i=1}^{2}(x_i^\alpha-x_i)\eta(x)_{,i}+\sum_{i=1}^{2}\sum_{j=1}^{2}\{(x_i^\alpha-x_i)(x_j^\alpha-x_j)/2\}\eta(\overline{x}^\alpha)_{,ij} \quad \cdots\cdots (22)$$

where $x=(x_1, x_2)$ is a point in the element, $\overline{x}^\alpha$ denotes a point on the line between x and x^α.

The interpolation function can be also written as follows using area coordinate L_α.

$$v_h(x)=\sum_{\alpha=1}^{3}\eta(x^\alpha)L_\alpha(x) \quad \cdots\cdots (23)$$

The area coordinate L_α can be expressed as (see **Fig. 2**):

$$L_\alpha=A_\alpha/A_e=a_\alpha+b_\alpha x_1^\alpha+c_\alpha x_2^\alpha \qquad (\alpha=1,2,3) \quad \cdots\cdots (24)$$

where

$$\left.\begin{aligned} a_\alpha&=(x_1^\beta x_2^\gamma-x_1^\gamma x_2^\beta)/2A_e\\ b_\alpha&=(x_2^\beta-x_2^\gamma)/2A_e\\ c_\alpha&=(x_1^\gamma-x_1^\beta)/2A_e \end{aligned}\right\} \qquad (\alpha, \beta, \gamma=1,2,3)$$

in which A_e is the area of the triangular element, which can be

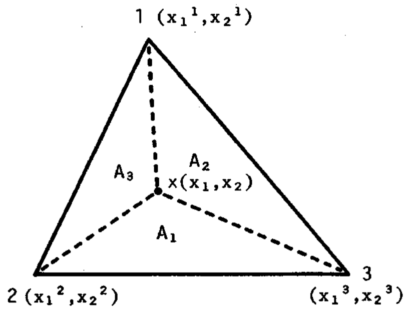

Fig. 2 Area coordinate.

computed as :

$$A_e=\{(x_1^\beta-x_1^\alpha)(x_2^\gamma-x_2^\alpha)-(x_1^\gamma-x_1^\beta)(x_2^\beta-x_2^\alpha)\}/2$$

And Using the partial (differentiation with respect to) x_j, the following equation can be obtained.

$$v_h(x)_{,j}=\sum_{\alpha=1}^{3}\eta(x^\alpha)L_\alpha(x)_{,j} \quad \cdots\cdots (25)$$

Introducing equations (23) and (25) into (22) and using the property of area coodinates, the following equations can be derived[19] :

$$\eta-v_h=\sum_{i=1}^{2}\sum_{j=1}^{2}\left[\sum_{\alpha=1}^{3}\{(x_i^\alpha-x_i)(x_j^\alpha-x_j)/2\}L_\alpha(x)\right]\eta(\bar{x}^\alpha)_{,ij} \quad \cdots\cdots (26)$$

$$(\eta-v_h)_{,i}=\sum_{i=1}^{2}\sum_{j=1}^{2}\left[\sum_{\alpha=1}^{3}\{(x_i^\alpha-x_i)(x_j^\alpha-x_j)/2\}L_\alpha(x)_{,i}\right]\eta(\bar{x}^\alpha)_{,ij} \quad \cdots\cdots (27)$$

Replacing η with η_h and introducing equations (26) and (27) into (20), it is possible to calculate the error measure E_e explicitly. However, the second derivative of η_h can not be computed because the linear interpolation function is used. Therefore, the continuious first derivative of η_h is computed by the least square method using the peacewise constant $\eta_{h,i}$ as follows :

$$\mathrm{Min}\sum_{e=1}^{Ne}\frac{1}{2}\int_\Omega(\hat{\eta}_{h,i}-\eta_{h,i})d\Omega \quad \cdots\cdots (28)$$

where $\hat{\eta}_{h,i}$ is the first derivative of η_h at nodal points. The second derivative of η_h can be obtained by the following equation.

$$\eta_h(x)_{,ij}=\sum_{\alpha=1}^{3}\hat{\eta}_{h,i}(x^\alpha)L_\alpha(x)_{,j} \quad \cdots\cdots (29)$$

(3) Solution Procedure of Adaptive Finite Element Analysis

The solution procedure of the adaptive finite element analysis based on the r-method is a sort of iterative method, the flow chart is shown in Fig. 3. The nodal points are relocated to satisfy the necessary condition, that is E_e=constant.

For the method of node relocation, the grid smoothing scheme introduced by Wilson[20] is modified, which is applied in the adaptive finite element analysis by Kikuchi et al. [12)~15)] Denoting the new coordinate x_p of nodal point P, which is relocated in accordance with the following equation (see Fig. 4) :

$$x_p=\sum_{e=1}^{Mn}(E_e/A_e^m)x_e\Big/\sum_{e=1}^{Mn}(E_e/A_e^m) \quad \cdots\cdots (30)$$

where M_n is the total number of elements which share the node P, and E_e, x_e, A_e are the error measure, the coordinate of the centroid, the area of such elements respectively, and m is a parameter for mesh smoothing. The hatched area shown in Fig. 4 indicates the limit of node relocation for one relocation. The node relocation based on the equation (30) was applied three times for one adaptation which means the application of the loop routine in the flow chart. For the parameter for mesh smoothing, m=0.5 was determined by several numerical experiments and used for all computation in this paper.

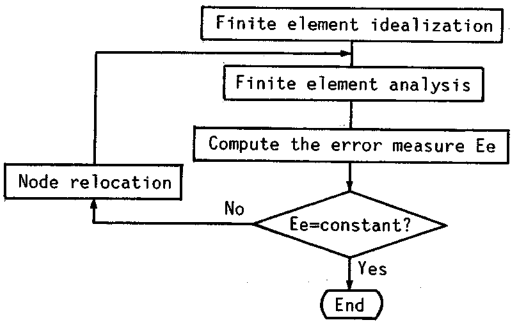

Fig. 3 Flow chart of adaptive finite element analysis.

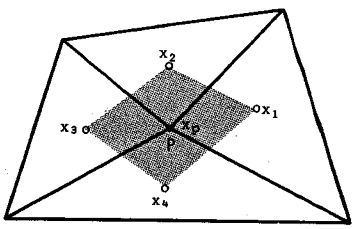

Fig. 4 Method of node relocation.

5. NUMERICAL TESTS

In order to show the validity of the present method, several numerical computations have been carried out comparing with the analytical solutions.

At the first example, consider a closed channel with constant water depth. Numerical computations have been performed impoing the wave number k which corresponds to the characteristic value of the channel. Fig. 5 shows the finite element idealization based on three node triangular element. For the boundary conditions, $\eta=1.0$ is prescribed on the boundary D–A and $\eta_{,n}=0.0$ is prescribed on the other boundaries. Fig. 6 shows the comparision between the computed and analytical wave form along the boundary A–B in case of the forth mode of this channel. In this figure, the solid line represents the analytical solution and the triangular mark is the finite element solution. Fig. 7 illustrates the distribution of error measure E_e. It

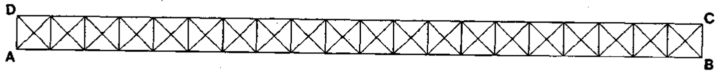

Fig. 5 Finite element idealization for a channel.

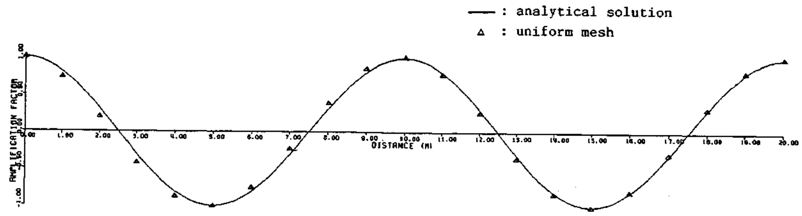

Fig. 6 Computed wave form in case of the forth mode.

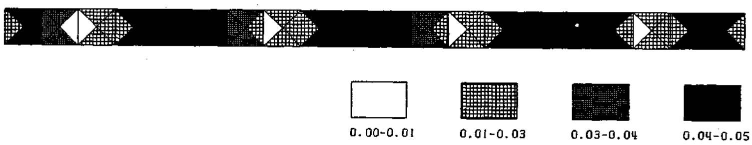

Fig. 7 Computed error measure E_e.

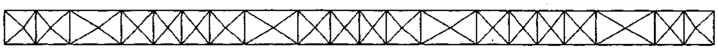

Fig. 8 Finite element idealization after two adaptations.

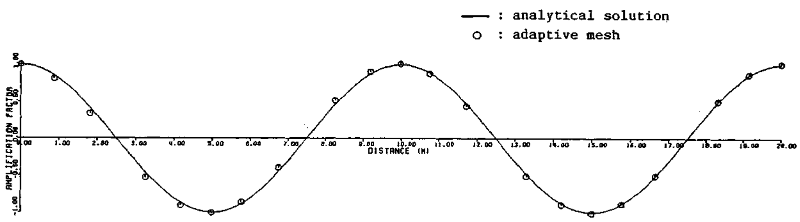

Fig. 9 Computed wave form.

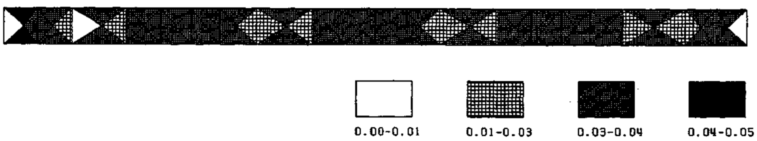

Fig. 10 Computed error measure E_e.

can be seen that the error measure at the wave antinode is larger than the other part. Fig. 8 is the new finite element idealization after two adaptations. The elements at the wave antinode are to be small according to the distribution of the error measure E_e. On the other hand, the elements at the other part are to be large because the variation of wave form is constant and the error measure is small. The circular mark in Fig. 9 shows the computed wave form using the finite element mesh which is shown in Fig. 8. Fig. 10 shows the error measure after two adaptations. It can be seen that the satisfaction of the necessary condition of the mesh optimization is better than the first results shown in Fig. 7.

The convergence property has been tested numerically as shown in Fig. 11, which represents the relation between the percentage error and the number of adaptations. The ordinate represents the percen-

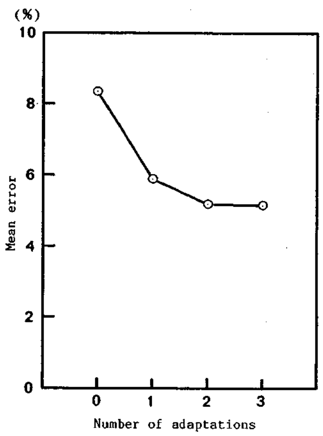

Fig. 11 Convergence property.

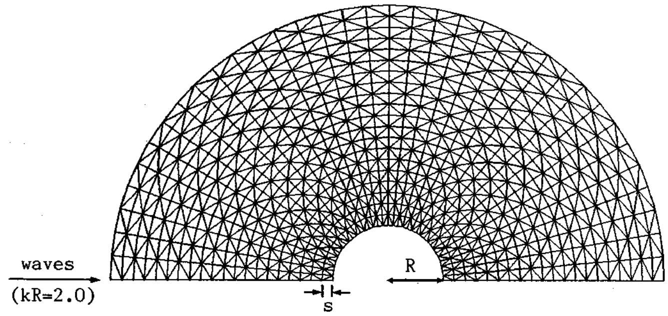

Fig. 12 Finite element idealization around a cylinder.

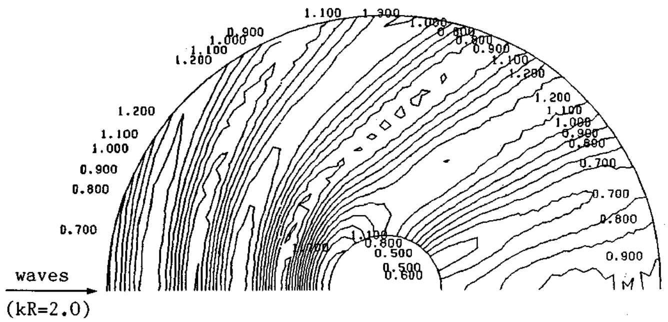

Fig. 13 Computed relative wave amplitude distribution.

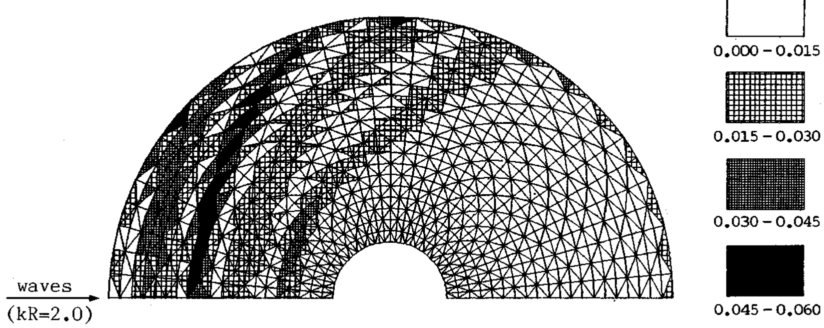

Fig. 14 Computed error measure E_e.

tage error and the abscissa is the number of adaptations. It can be seen that the numerical accuracy is converged by two adaptations, and is improved automatically by using the adaptive mesh refinement technique.

As the second example, the present method is applied to the wave diffraction problem by a circular cylinder. Fig. 12 represents the half of the finite element idealization around a cylinder. The total number of elements and nodes are 2 880 and 1 512 respectively. The water depth is assumed to be constant and the wave number is chosen to be $kR=2.0$, where R is the radius of the cylinder. In this case, the ratio between element length s and wave length $L(s/L)$ is 1/15.7. The computed relative amplitude distribution is illustrated in Fig. 13. Fig. 14 shows the computed error measure E_e. It can be seen that the error measure at the wave node and antinode is large. Fig. 15 is the new finite element idealization after one adaptation using the results of the computed error measure. Fig. 16 is the computed relative wave amplitude distribution using the finite element idealization shown in Fig. 15. The computed results obtained by the present method are compared with the analytical solution solved by MacCamy and Fuchs[21]. Fig. 17 illustrates the comparison on the body surface of the cylinder. In this figure, the solid line represents the analytical solution, the triangular mark is the computed results using the initial mesh shown in Fig. 12, and the circular mark represents the computed results using the adaptive mesh shown in Fig. 15. It can be seen that the computed results using the adaptive mesh refinement technique are in good agreement with the analytical solution as compared with the results using initial mesh. The computational time involving the one adaptation was 30 second using HITAC M 680 H of University of Tokyo.

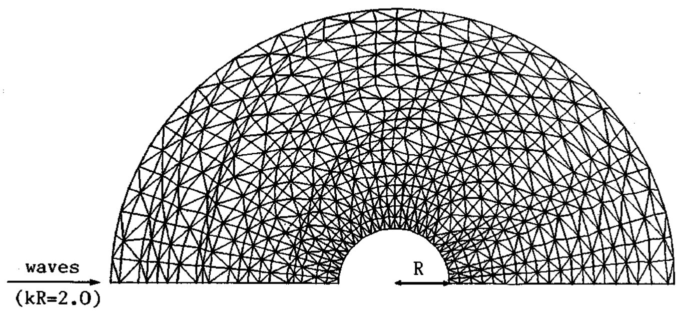

Fig. 15 Finite element idealization after one adaptation.

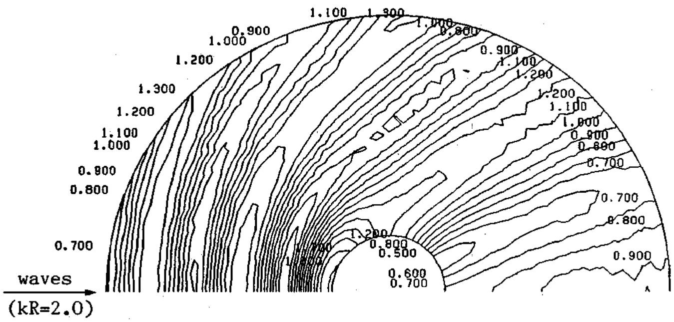

Fig. 16 Computed relative wave amplitude distribution.

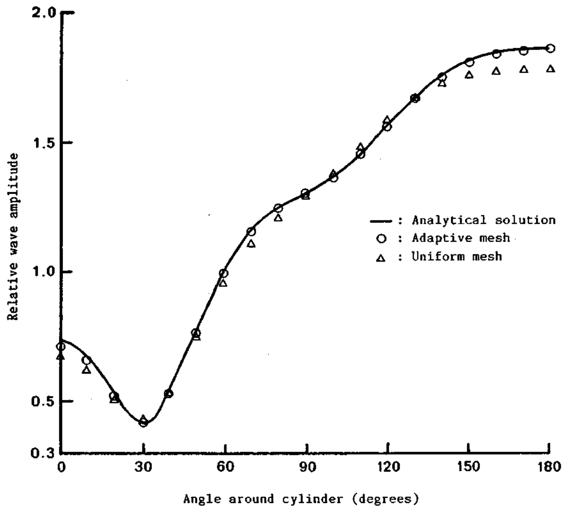

Fig. 17 Comparison between computed and analytical solutions on a circular cylinder.

6. CONCLUSION

An adaptive finite element method based on the r-method has been presented in this paper for the analysis of linear water wave problems. The key feature of this method as compared with the conventional numerical methods are as follows. The approximation error can be estimated in each finite element. And the finite element mesh can be redivided to minimize the approximation error. These follows that the numerical accuracy can be improved automatically.

The computed results obtained by the present method have been compared with existing analytical solution. From these comparative studies, the solution obtained by the present method is assured to be satisfactorily close to the analytical solution. Moreover, the coarser finite element mesh idealization is adaptable than those employed in conventional finite element method. The present method will be applied to the more actual problems in the future work.

ACKNOWLEDGEMENT

The authors wish to express their gratitude to Dr. Noboru Kikuchi, professor of University of Michigan, and to Dr. Masahiko Isobe, associate professor of Yokohama National University, and to Dr. Fumio Kikuchi, associate professor of University of Tokyo, and to Dr. Masayuki Okabe, Mitsui Mining & Smelting Co., Ltd., for their useful suggestions and discussions.

This research was, in part, supported by a Grant in Aid in Engineering and Science of Ministry of Education of Japan, No. 60550330.

REFERENCES

1) Berkhoff, J. C. W. : Computation of combined refraction-diffraction, Proc. 13th Int. Conf. Coastal. Eng., ASCE, pp. 471~490, 1972.
2) Chen, H. S. and Mei, C. C. : Oscillations and wave forces in an offshore harbor, Ralph M. Persons Lab., MIT, Report No. 190, 1974.
3) Bettess, P. and Zienkiewicz, O. C. : Diffraction and refraction of surface waves using fihite and infinite elements, Int. J. Numer. Methods Eng., Vol. 11, pp. 1271~1290, 1977.
4) Houston, J. R. : Combined refraction and diffraction of short waves using the finite element method, Appl. Ocean Res., Vol. 3, pp. 163~170, 1981.
5) Tsay, T. K. and Liu, P. L-F. : A finite element model for wave refraction and diffraction, Appl. Ocean Res., Vol. 5, pp. 30~37, 1983.
6) Kashiyama, K. and Kawahara, M. : Boundary type finite element method for surface wave problems, Proc. JSCE, No. 363/2, pp. 205~214, 1985.
7) Chen, H. S. : Effects of bottom friction and boundary absorption on water wave scattering, Appl. Ocean Res., Vol. 8, pp. 99~104, 1986.
8) for example, Accuracy Estimates and Adaptive Refinements in Finite Element Computation, (Eds. Babuska, I., Zienkiewicz, O. C., Gago, J., and Oliveira, E. R. de A.), Wiley, New York, 1986.
9) Smith, R. and Sprinks, T. : Scattering of surface waves by a conical island, J. Fluid Mech., Vol. 72, part 2, pp. 373~384., 1975.
10) Mei, C. C. : The Applied Dynamics of Ocean Surface Waves, Wiley, New York, 1983.
11) Booij, N. : A note on the accuracy of the mild-slope equation, Coastal Engineering, Vol. 7, pp. 191~203, 1983.
12) Diaz, A. R., Kikuchi, N., and Taylor, J. E. : A method of grid optimaization for finite element methods, Comp. Meth. Appl. Mech. Eng., Vol. 37, pp. 29~46, 1983.
13) Kikuchi, N. and Diaz, A. R. : Finite element approximation of Navier/Stokes flow problems using grid optomization methods, Proc. 5 th Conf. Finite Elements and Flow Problems, pp. 41~47, 1984.
14) Kikuchi, N. : Adaptive grid design methods for finite element analysis, 2nd Joint ASCE/ASME Mech. Conf., 1985.
15) Kikuchi, N. : Adaptive grid design for finite element analysis in optimization ; Prat 1. Review of finite element error analysis, Part 2. Grid optimization, (in press).
16) Babuska, I. and Rheinboldt, W. C. : A-posteriori error estimates for finite element method, Int. J. Numer. Methods Eng., Vol. 12, pp. 1597~1615, 1978.
17) Babuska, I. and Rheinboldt, W. C. : Error estimates for adaptive finite element computations, SIAM J. Numer. Anal., Vol. 15, pp. 736~754. 1978.
18) Babuska, I., Szabo, B. A. and Katz, I. N. : The p-version of the finite element method, SIAM, J. Numer. Anal., Vol. 18, pp. 515~545, 1981.
19) Kikuchi, F. and Okabe, M. : An Introduction of Finite Element Systems, Chpter 11, JUSE, 1986 (in Japanese).

20) Wilslow, A. : Numerical solution of the quasilinear Poisson equation, J. Comp. Phy., Vol. 1, pp. 149~172, 1966.
21) MacCamy, R. C. and Fuchs, R. A. : Wave forces on a pile ; a diffraction theory, Tech. Memo, No. 69, U. S. Army Corp. Eng., 1954.

(Received December 22 1986)